Available online at www.sciencedirect.com
ScienceDirect
Journal of Molecular Graphics and Modelling 25 (2007) 903–911
Journal of Molecular Graphics and Modelling
www.elsevier.com/locate/JMGM

The molecular dynamics of assembly of the ubiquitous aortic medial amyloidal medin fragment

Ehud Gazit [a], Paola della Bruna [b], Stefano Pieraccini [b], Giorgio Colombo [b,*]

[a] Department of Molecular Microbiology and Biotechnology, George S. Wise Faculty of Life Sciences, Tel Aviv University, Tel Aviv 69978, Israel
[b] Istituto di Chimica del Riconoscimento Molecolare, CNR, Via Mario Bianco 9, 20131 Milano, Italy

Received 14 March 2006; received in revised form 1 September 2006; accepted 1 September 2006
Available online 8 September 2006

Abstract

In recent years there is an increased understanding of the molecular conformation of amyloid fibrils. However, much less is known about the early events that lead to the formation of these medically important assemblies. The clarification of these very important mechanistic details on the process may indicate directions towards the inhibition of the early stages of the assembly, where harmful species are most likely to form. Here, we study the dynamics of assembly of short amyloidogenic peptide fragments from the medin polypeptide. This polypeptide is of unique interest since amyloid deposits composed of medin are found almost in all the population above the age of 50. Twelve independent 50 ns long molecular dynamics simulations in explicit water have been run on peptide NH_2–NFGSVQFV–COOH, the minimal recognition hexapeptide element, NH_2–NFGSVQ–COOH, and several single-point mutants. In all cases a three-stranded polymeric β-sheet was used as the basic unit from which fibrils can be formed. Our results clearly indicate the need of well-defined sequence and stereochemical constraints to allow the formation of stable well-ordered aggregates. One of the key findings is the need for the presence of a phenylalanine residue, but not other hydrophobic amino acids, in specific positions within the peptide. Taken together, the results are consistent with recent high-resolution structures of amyloid assemblies and provide unique insights into the dynamics of these structures.

Keywords: Amyloid fibril formation; Molecular dynamics; Aortic medial amyloid; Aromatic interaction; Molecular recognition; Protein misfolding; Self-assembly

1. Introduction

The accumulation of amyloid fibril deposits is associated with a large number of diseases of unrelated origin affecting humans and animals. This amyloid-associated disorder ranges from neurodegenerative disease, such as Alzheimer's disease and spongiform encephalopaties, to metabolic and systemic diseases including type II diabetes to several familial amyloidosis conditions [1,2]. Moreover, the ability to form amyloid assemblies is not only restricted to disease-related proteins. There are already large numbers of non-pathogenic peptides and proteins that have been shown to form typical amyloid fibrils under particular solvent, pH and temperature conditions [3–5]. Fibril formation may also be a normal physiological phenomena in various microorganisms, as it role in the formation of biofilm and aerial hyphae was demonstrated [6,7]. Fibril formation represents a case of self-recognition process in which the deposition of aggregates is linked to a structural rearrangement of proteins or polypeptides from their monomeric, correctly folded, functional and soluble structures to insoluble ones with a predominant β-sheet secondary structure.

The observation of common structural properties for the final amyloidal deposits that are formed by proteins with very different sequences, has led to the view that the propensity to form amyloid fibrils is a general property of the polypeptide backbone [3–5], suggesting that at infinite time any protein solution above a critical concentration may eventually undergo structural transition into the aggregated state [8]. On the other hand, several studies have shown that the propensity of a certain polypeptide chain to aggregate depends dramatically on amino acid composition and that, therefore, specific side-chain residues actually influence the rate of formation and the stability of amyloid assemblies. As a consequence, specific

* Corresponding author. Tel.: +39 02 28500031; fax: +39 02 28500036.
E-mail address: giorgio.colombo@icrm.cnr.it (G. Colombo).

1093-3263/$ – see front matter
doi:10.1016/j.jmgm.2006.09.001

molecular recognition elements come into play and regulate the fibril formation process [9–12].

In this context, the study of the aggregation propensities of short peptide sequences that retain all the molecular information needed to undergo fast and efficient fibril formation represents a very useful reductionist approach to shed light on the specific molecular details that underlie this process: the use of minimal fibril forming sequences may allow the effects of the perturbation of single properties on aggregation to be pinpointed. Small-sized systems are extremely useful not only at the experimental level but also at the theoretical one. Theoretical and computer-based approaches in fact offer the possibility to overcome the problems opposed by the insoluble and intractable character of amyloid aggregates to their characterization at atomic level via conventional biophysical techniques. Molecular dynamics (MD) simulations, in particular, have been recently shown to be very useful for dissecting the factors leading to spontaneous assembly of Aβ-peptides into antiparallel β-sheets [13], investigating the tendency of monomeric peptide units to populate β-type structures [14], the kinetics and mechanisms of the self-assembly process [15–20], the structural and sequence determinants that govern the very early steps of amyloid fibril formation and the effect of chaotropic agents such as urea on the stability of oligomers [17,21–26].

Many of these experimental and theoretical studies have highlighted the importance of intermolecular aromatic interactions in the stabilization of short model peptides ranging from the 5F mutant of the designed STVIIE sequence to the fragments derived from the islet Amyloid polypeptide such as NFGAIL and FGAIL. In the latter case, it was shown that only the substitution of phenylalanine (Phe), and not of any other residue, by alanine (Ala) was able to completely abolish fibril formation [27]. The fundamental role of Phe was also highlighted by MD simulation studies of the initial stages of aggregation in a concentrated microscopic model. The same role was observed for instance in peptides derived from calcitonin and other proteins. Recent high-resolution studies of amyloid assemblies provided a direct evidence for the role of aromatic interactions in many cases of amyloid formation [28–30]. These NMR and X-ray diffraction studies have a pivotal importance in the path for the understanding of the structure of the amyloid assemblies. Yet, further information is needed on the dynamics that leads to the formation of these highly ordered assemblies. The understanding of the dynamics process is not only important from the mechanistic point of view but should provide new insights for the design of inhibitors that may control this process.

To further investigate the dynamics of amyloid self-assembly, the role of aromatic/hydrophobic recognition versus backbone interactions, and to test against experiments and generalize the results of previous MD studies on related sequences [18,26], we became interested in the study of the short amyloidogenic octapeptide (NH_2–NFGSVQFV–COOH) derived from medin, and of its truncated and mutated analogues [27]. Medin is the main constituent of aortic medial amyloid deposits. Aortic medial amyloid was found in 97% of the subjects above the age of 50 [31]. However, the pathological role of those amyloid deposits is still unclear. It was suggested that these deposits can diminish the elasticity of aortic vessels that is related to old age [31]. Previous studies allowed the determination of the minimal sequence of the peptide necessary to induce amyloid fibril formation [27]. However, much remains to be unveiled in the case of the molecular determinants that mediate the process of amyloid formation.

Table 1
Simulated sequences, starting conformations and simulation labels

Sequence	β-Sheet orientation	Simulation label
NH_2–NFGSVQFV–COOH	Parallel	*Medin_8_par*
NH_2–NFGSVQFV–COOH	Antiparallel	*Medin_8_anti*
NH_2–N**I**GSVQ**I**V–COOH	Parallel	*8_Ile_par*
NH_2–N**I**GSVQ**I**V–COOH	Antiparallel	*8_Ile_anti*
NH_2–N**A**GSVQ**A**V–COOH	Parallel	*8_Ala_par*
NH_2–N**A**GSVQ**A**V–COOH	Antiparallel	*8_Ala_anti*
NH_2–NFGSVQ–COOH	Parallel	*Medin_6_par*
NH_2–NFGSVQ–COOH	Antiparallel	*Medin_6_anti*
NH_2–N**I**GSVQ–COOH	Parallel	*6_Ile_par*
NH_2–N**I**GSVQ–COOH	Antiparallel	*6_Ile_anti*
NH_2–N**A**GSVQ–COOH	Parallel	*6_Ala_par*
NH_2–N**A**GSVQ–COOH	Antiparallel	*6_Ala_anti*

To shed light on these factors, we have performed a systematic all-atom MD analysis of the effects of the sequence mutation, sequence length and relative orientation of the constituent β-strands on the stability of minimal polymeric β-sheet structures similar to those assumed to be present in amyloid fibrils. Here, we have considered a three-stranded polymeric β-sheet as the elementary unit from which amyloid fibrils can assemble. This approximation is based on the fact that β-sheets of this size have already been shown to be appropriate as structural templates for the design of sequences that polymerize into β-sheets and further form amyloid fibrils [26], and on the observation by Eisenberg and co-workers that three molecules may represent the transition state on the path to the nucleus of a protofibril [32]. On this basis, 12 different 50 ns long MD simulations in explicit water have been run on peptide NH_2–NFGSVQFV–COOH, its truncated hexapeptide form, NH_2–NFGSVQ–COOH, and several single-point mutants [27] (see Table 1, reporting different mutants and simulation labels) starting from single three-stranded β-sheets of different conformation (parallel or antiparallel strand arrangement; Fig. 1a–d). The analysis of the stabilizing or destabilizing effect of particular mutations on oligomeric β-sheets has provided evidence for the critical role of specific side-chain interactions in the stabilization of nascent aggregates, and thereby for the origin of the specific molecular recognition effects on β-sheet polymerization and fibril formation that were found experimentally for this system.

2. Methodology

Two different conformational templates were used for the simulations: one represents a three-stranded β-sheet arrangement of hexapeptides in antiparallel conformation and the other represents the same hexapeptides in a parallel disposition. The

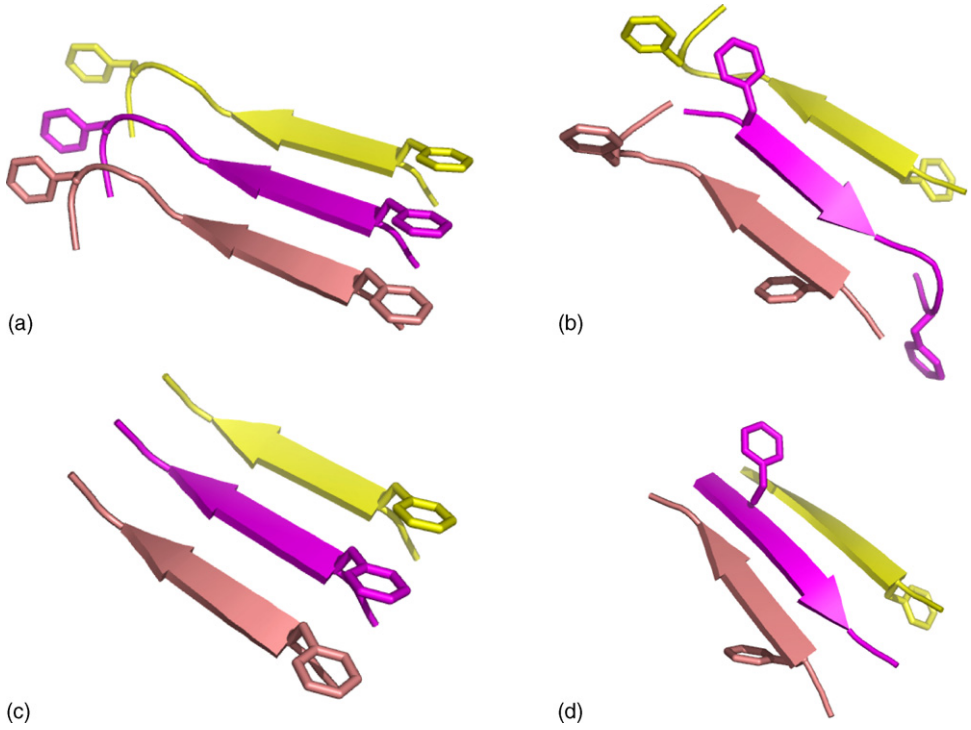

Fig. 1. Starting structures for the MD simulations of the original and truncated medin sequences: (a) *Medin_8_par*; (b) *Medin_8_anti*; (c) *Medin_6_par*; (d) *Medin_6_anti*. The positions and side chains of Phe residues are highlighted.

simulations, their starting conformations, sequences and labels are reported in Table 1. The starting structures are depicted in Fig. 1. The charge conditions were set to mimic the solution conditions at pH 7. Each simulated sequence resulted to bear a total charge of zero, so that no counter ions were used in the simulations.

The three stranded β-sheets were solvated with water in an octahedral box large enough to contain 1.2 nm of solvent around the peptide. The simple point charge (SPC) water model was used [33] to solvate each complex in the simulation box. Each system was subsequently energy minimized with a steepest descent method for 1000 steps. The calculation of electrostatic forces utilized the twin range cutoff method (0.8 nm for van der Waals interactions and 1.4 nm for electrostatics). The LINCS [34] algorithm was used to constrain all bond lengths. For the water molecules the SETTLE algorithm [35] was used. A dielectric permittivity, $\varepsilon = 1$, and a time step of 2 fs were used. All atoms were given an initial velocity obtained from a Maxwellian distribution at the desired initial temperature of 300 K. The density of the system was adjusted performing the first equilibration runs at NPT condition by weak coupling to a bath of constant pressure ($P_0 = 1$ bar, coupling time $\tau_P = 0.5$ ps) [36]. In all simulations the temperature was maintained close to the intended values by weak coupling to an external temperature bath [36] with a coupling constant of 0.1 ps. The peptide and the rest of the system were coupled separately to the temperature bath.

In all cases, the peptides were simulated at 310 K for 50 ns. All simulations were run at NPT conditions.

All simulations and analysis were carried out using the GROMACS package (version 3.2) [37,38], using the GROMOS96 43A1 force field [39]. In the calculations of the contact matrices (Figs. 6 and 7) the average matrix is calculated averaging over the whole trajectory, while the ones corresponding to the 10 ns time windows have been calculated only at time windows of 10 ns each. All calculations were performed on clusters of PCs, with Linux operating system. Graphical display of structures was done using the PyMOL software. Structural clusters were defined using the structural clustering algorithm proposed by Daura et al. [40].

3. Results and discussion

The cross-β-structure inferred from X-ray diffraction data on a series of amyloid fibrils is compatible with either a parallel or an antiparallel arrangement of the of the polypeptide strands. The relative orientation of single strands depends on the sequence of the polypeptide and on the type of interactions between single strands. In the case of Aβ(16–22) for instance, Gordon et al. suggested that increasing the amphiphilicity of the peptide can result in a switch from parallel to antiparallel of the β-sheet structure [41]. To take into consideration the different relative orientation of the strands, we have considered two different β-sheet conformations as starting points for each sequence: a parallel and an antiparallel one. The stability of the starting conformation during the simulations was estimated by monitoring the time evolution of the content of ordered β-sheet structure. Fig. 2 clearly shows that for the original octapeptide and for its truncated hexameric form, the parallel orientation of the strands used in simulations labeled *Medin_8_par* and *Medin_6_par* determines a global conservation of the ordered β-sheet secondary motif over the whole timescale of the

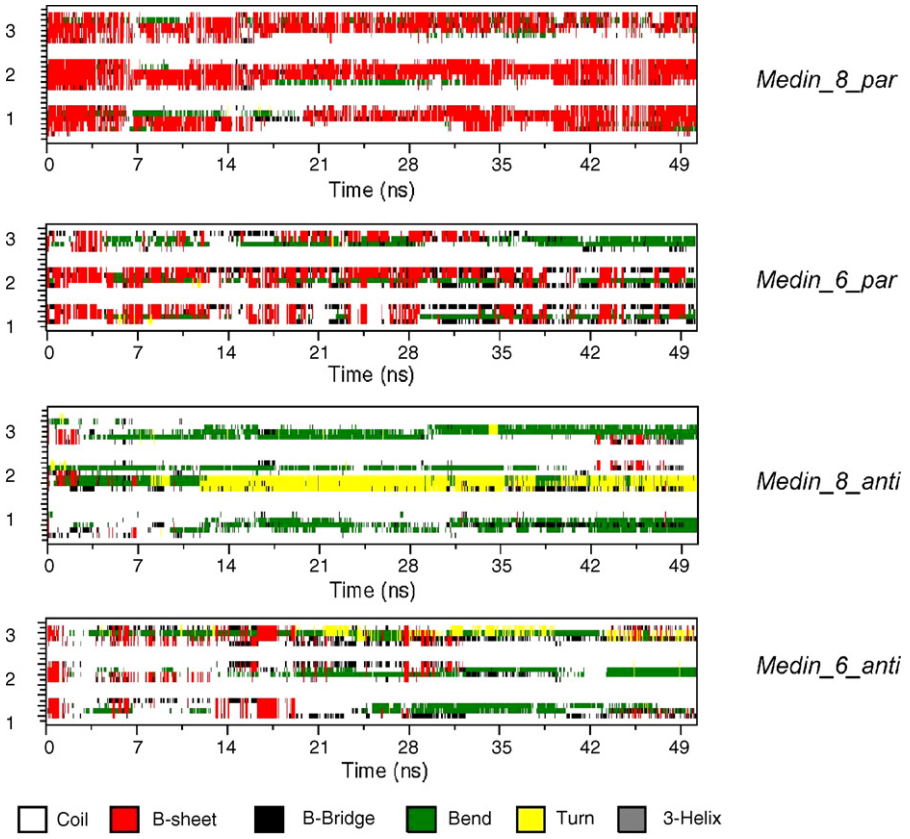

Fig. 2. Time evolution of the secondary structure of the original and truncated medin sequences in the different simulations starting from different initial conformations.

simulation. In contrast, the simulation of three antiparallel chains (*Medin_8_antipar* and *Medin_6_antipar*) determines a rapid loss of interchain hydrogen bonding both in the octapeptide and in the hexameric truncated form of the original sequence. In neither of these cases, did we observe a complete conformational transition leading from the antiparallel to the parallel arrangement, as should be expected considering the limited timescale of our simulations. However, it is worth noting that a rearrangement to a parallel double stranded β-sheet could be observed towards the end of simulation *Medin_8_antipar*, bringing two Phe groups in close proximity to form a small aromatic patch.

Related MD studies on other different short sequences, namely, STVIIE and its mutants, revealed a preference for the antiparallel versus the parallel arrangement [26]. These peptides were however characterized by the presence of uncompensated net charges at the terminals, used to mimic the experimental conditions. In such short sequences, net charges on the peptides play a fundamental role in favoring a supramolecular organization in which the distance between charges of the same sign is maximized. At the β-sheet level, it may favor the antiparallel versus the parallel conformation, or even prevent the formation of the nascent aggregate. In contrast, in the case of medin derived peptides, net uncompensated charges are not present on the sequences in consonance with experimental conditions, so that peptide assembly is mainly driven by other sequence-dependent factors. The stability of the parallel arrangement of *Medin_8_par* and *Medin_6_par* may be mainly ascribed to the presence of favorable Phe–Phe interactions (Fig. 3a–c). Phe combines a high β-sheet propensity with the possibility to form a number of interstrand hydrophobic and aromatic (stacking) interactions. This is particularly true for the case of the parallel octapeptide sequence in which the presence of two Phe groups per strand, combined with the L-absolute configuration of these residues, determines the formation of two ordered and stable hydrophobic patches. In the truncated *Medin_6_par* only one of the two Phe is still present in the sequence, resulting in the possibility to form only one ordered aromatic patch. This is enough to stabilize the nascent protofibril, although to a slightly lower extent. It is worth noting that the 3D structures representative of the most populated cluster for simulation *Medin_8_par* display an *edge-to-face* packing of the phenyl rings of Phe on consecutive strands. In the case of the representative conformation of the second cluster, the packing of Phe residues is *face-to-face*. Cluster 1 accounts for around 65% of all the structures found, while cluster 2 accounts for around 25%. The situation is reversed in the case of *Medin_6_par*, where however the two most populated cluster account for 40 and 25% of the total population, respectively. These two different types of packing for aromatic rings are well known to be the most stabilizing ones, also in the context of protein and peptide conformational stabilization.

The antiparallel conformation of *Medin_8_anti* and *Medin_6_anti* prevents the aromatic patch to be formed, because of unfavorable stereochemical constraints. In an ideal antiparallel conformation, the side-chains of Phe flanking each other would point towards opposite directions in space. This has severe

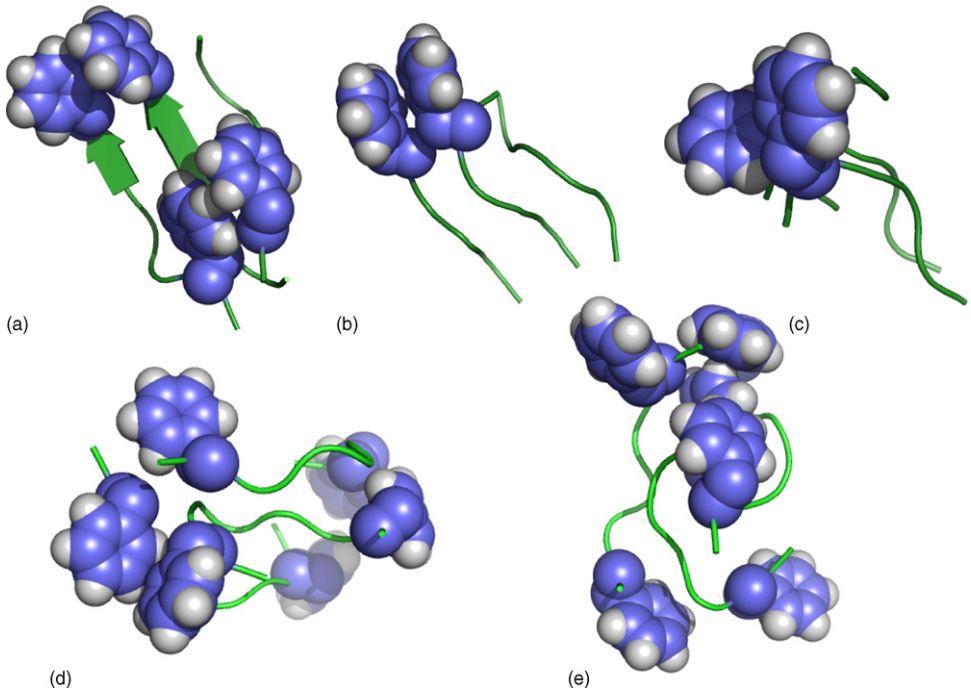

Fig. 3. Stabilizing packing of the side chains of Phe in the representative structure of the most populated cluster for *Medin_8_par* (a) and for the representative structures of the first and second most populated clusters for *Medin_6_par* (b) and (c). The edge-to-face packing in the 8 residue peptides should be noticed, while the face-to-face and edge-to-face packing types are present for the 6-residue analog.

consequences in terms of stability, at least on the timescales that we have used here. In particular, Fig. 3d and e exemplify the situation due to an antiparallel arrangement showing the conformations of the representatives of the two main structural clusters of the *Medin_8_anti* simulation. It is clear that no ordered packing of Phe side chains can be observed here, and that the backbone shows no particular secondary structure feature. The only contacts form between Phe side chains (edge-to-face) only when one of the strands leaves the starting extended conformations and folds into a more compact one, as can be observed in the second structural cluster (Fig. 3e). This particular state is obviously not convenient for the formation of an ordered fibril, and represents a conformational trap in our simulations. At this stage of simulation, however, we cannot rule out a transition

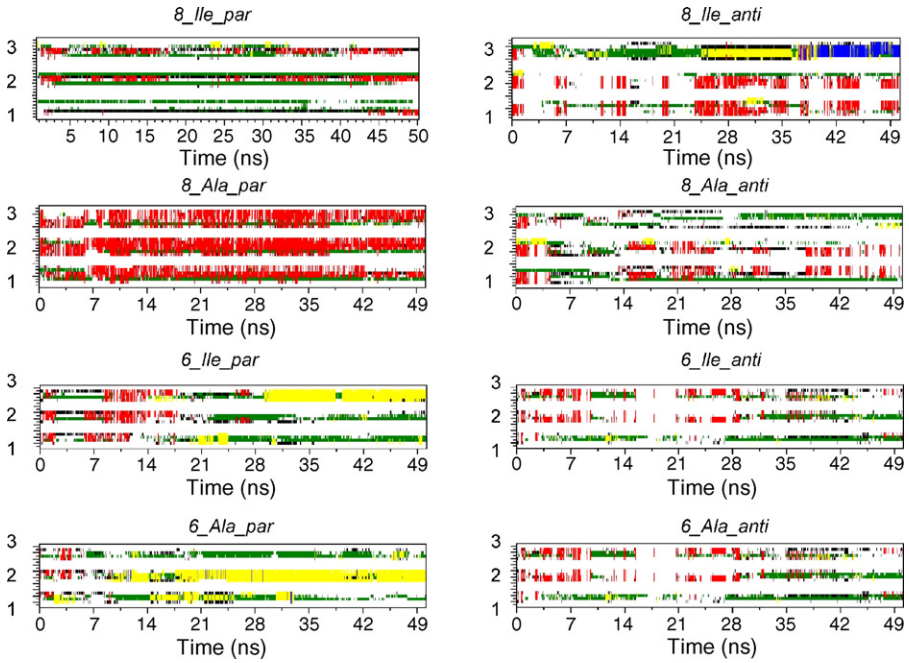

Fig. 4. Time evolution of the secondary structure of the 8- and 6-residue long mutants of medin sequences in the different simulations starting from different initial conformations.

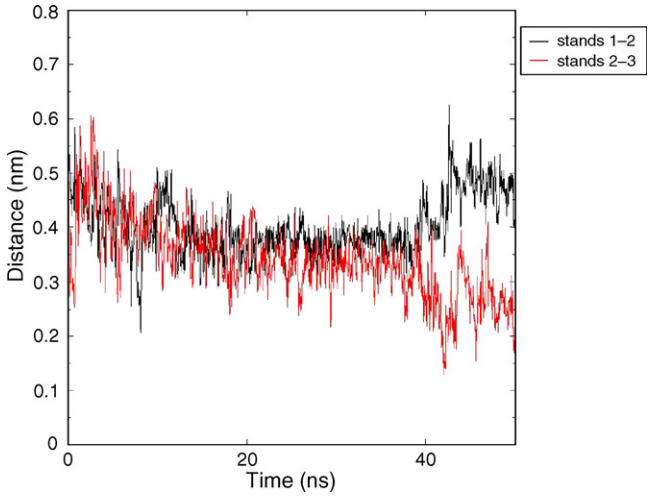

Fig. 5. Time evolution of the distance between the centers of mass of adjacent strands in the *8_Ala_par* simulation. A reduction of the interstrand distance with time can be noticed.

between the antiparallel and the parallel arrangement. The simulations time scales that we can access now with all atom models simply do not allow us to observe this event.

Energetically, the parallel arrangement results more stable. The Lennard–Jones interaction energy between two consecutive strands in the *Medin_8_par* simulation is -138.30 ± 19.34 kJ/mol, while in the case of the *Medin_8_anti* simulation, this value is sensitively higher and results -120.35 ± 18.00 kJ/mol. In contrast, the Coulombic interactions between consecutive strands display very similar values of -1.58 ± 2.14 kJ/mol for *Medin_8_par* and -1.56 ± 4.30 kJ/mol for *Medin_8_anti*. This analysis shows one more that interactions mainly due to hydrophobic interactions: Phe–Phe is not only hydrophobic, but also has the ordering and directionality properties, which are suitable to stabilize ordered oligomers.

The effect of sequence on the stability of the three-stranded polymeric β-sheet elementary unit was subsequently analyzed by mutating Phe residues to either Ile or Ala, still starting from two different initial conformations of the β-sheets, antiparallel and parallel. The stability of the mutated elementary units in MD simulations was once more benchmarked against experimental results on fibril formation.

MD simulations show that Ala and Ile substitution induce a complete loss of the three stranded β-sheet ordered secondary structure during the simulation time when starting from the antiparallel arrangement, both for the case of the octapeptide (with two substitutions) and for the case of the hexapeptide (with one substitution) (see Fig. 4).

When considering the parallel arrangements, the truncated Ala or Ile containing hexapeptides rapidly loss their initial

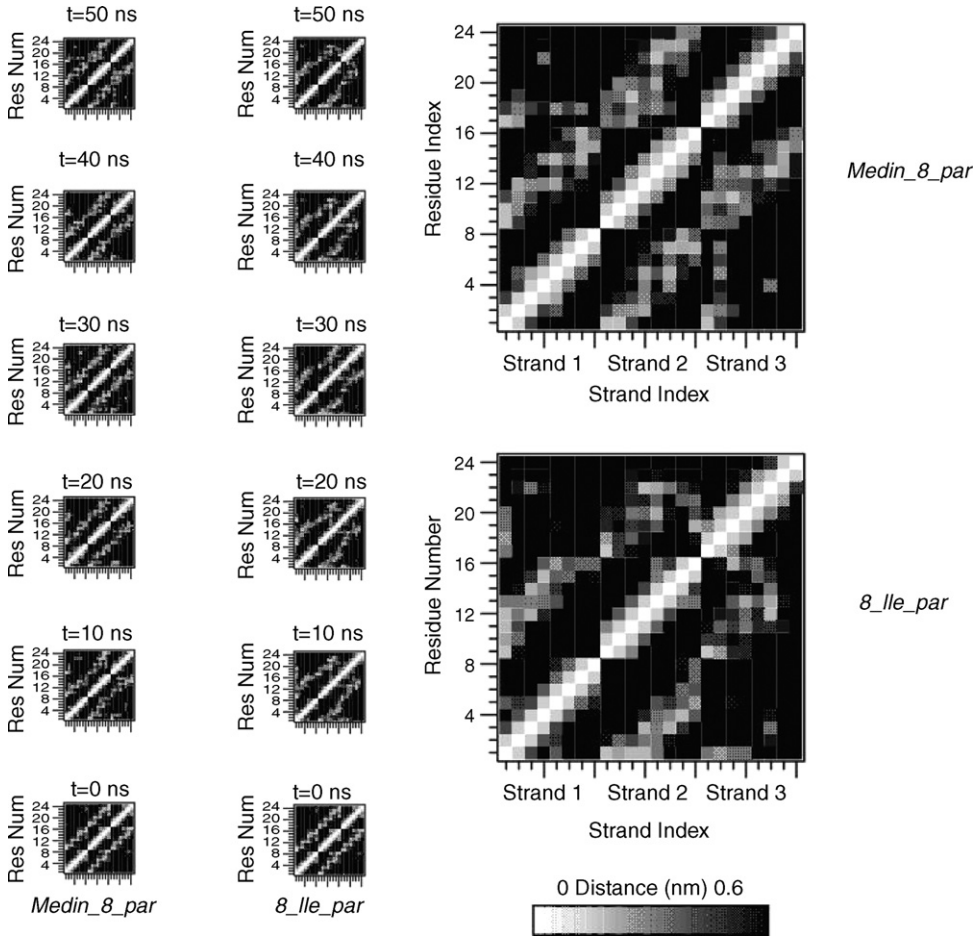

Fig. 6. Left panel: time evolution of the intermolecular contacts in *Medin_8_par* and *8_Ile_par*. Right panel: average contact maps for the two simulations.

β-sheet conformation. In the case of the octapeptide carrying two Phe to Ile substitutions (simulation *8_Ile_par*), a small percentage of the initial ordered β-structure involving only two strands survives for about 50% of the simulation, mainly due to hydrophobic interactions involving the side chain of Ile. In contrast, the substitution of the two Phe to Ala in the parallel arrangement of the octapeptide results in a net conservation of the β-sheet structure, at least in the 50 ns timespan of the MD simulations. Experimentally, it was observed that substitutions to Ala could still yield some degree of Congo Red birefringence, suggesting the presence of ordered amyloid fibrils [27]. The higher stability of the template in this case may be due to the fact that Ala is a good β-sheet former with a very limited steric hindrance of the side chain. This in turn allows to adjacent strands to become closer than in the other two cases (see Fig. 5) and form a productive number of in register interstrand hydrogen bonds. This is not observed in the case of the truncated hexapeptide (*6_Ala_par*), where the number of hydrogen bonds that can potentially form is not enough to overcome the loss of aromatic stabilization due to the mutation of Phe.

The observations and simulation results presented above, suggest that the stability of fibril nuclei and their supramolecular organization are determined by a combination of factors, namely, the relative orientation of single strands and the presence and orientations of particular side chains. In particular, we noticed that the presence of Phe residues in positions 2 and 6 of the original medin sequence (NH_2–NFGSVQFV–COOH) and in position 2 of the truncated hexapeptide sequence (NH_2–NFGSVQ–COOH) in parallel conformation strongly stabilizes a three-stranded β-sheet structure, which can act as a nucleus for the growth of a fibril. Interestingly, substitution of Phe to Ile, with a hydrophobic and sterically hindering side chain, clearly decreases or even abolishes (for the hexamer case) the degree of ordered β-structure. Not only this is consistent with experimental observations on this particular sequence, but also with other observations on short peptide fragments, for which it was shown that there is no correlation between simple hydrophobicity and amyloidogenic potential. The side chain of Phe, due to the planarity of its aromatic ring, can in fact achieve a much more favorable packing situation than in the case all other non-aromatic hydrophobic residues. In this line of thought, energy analysis shows that *Medin_8_par* is much more stable than its antiparallel counterpart. This is not observed for any of the other cases. Interestingly, the presence of two Ala substitutions in *8_Ala_par* seems to still favor the stabilization of the fibril nucleus, although the number of intermolecular

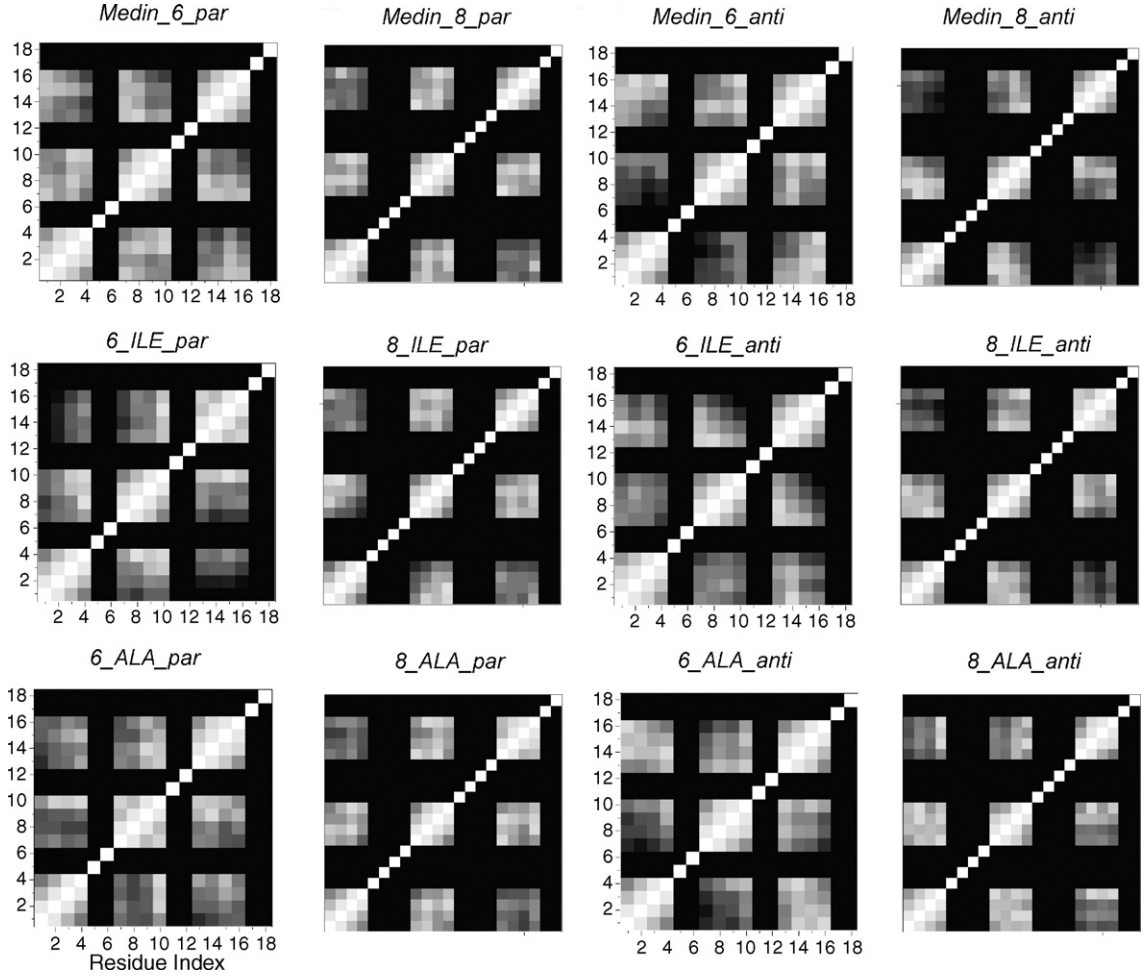

Fig. 7. Average contact maps, calculated over the whole simulation lengths, of the central residue stretch GSQV for all sequences and simulations.

contacts is lower than in the other cases. The limited steric hindrance of Ala allows the two backbones of the 8-membered chains to establish enough interchain hydrogen bonds to stabilize the parallel conformation. This does not happen in the truncated or antiparallel conformations, where an optimal number or an optimal alignment of hydrogen bonds cannot be obtained.

The important role of Phe–Phe aromatic interactions is underlined also by the analysis of the time evolution of contact maps. Two residues are considered to be in contact if the distance between any two atoms belonging to either residue is lower than 6.0 Å. It is evident that, e.g. in the case of *Medin_8_par* the typical contact pattern of parallel strands is conserved for the whole simulation time (Fig. 6). When *8_Ile_par* is considered, in contrast, the elements parallel to the main diagonal of the contact matrix, a signature of parallel β-sheets, are frayed after 10 ns, starting from the C-terminal of strand 2 and N-terminal of strand 3, where the substitution to Ile has been introduced (Fig. 6). In this case, the side chain of Ile is involved in several contacts, with a lower degree of order than the ones in the Phe analogs. The same holds also for the other cases studied, where disassembly of the nucleus occurs (see Fig. 6). Fig. 7 shows the average contact matrices calculated in all the simulations only for the GSVQ stretch of residues, which is shared by all the sequences analyzed herein. These data show that there are no appreciable differences among the contact maps of the common sequence, in spite of the very different behavior observed for the secondary structure and energetic evolution. These data once more strengthen our idea regarding the important role of Phe–Phe in stabilizing the nascent aggregate and providing the proper degree of spatial ordering to the growing fibril.

4. Conclusions

The current study provides new insights into the highly important mechanism of amyloid fibril formation. The MD study using explicit solvent performed in this work clearly demonstrates that the stability of a model nucleus of a fibril is determined by a combination of factors, namely, the sequence identity and relative disposition–orientation of aromatic side-chains. In particular, the presence of the aromatic Phe residue at well-defined positions and with well-defined stereochemical orientation in space is the key determinant for the stabilization of the three-stranded amyloidal unit. The analysis of the effect of some substitutions has provided additional evidence for the influence of site-specific side chain interactions showing once again that sequence identity determines the tendency to form in ordered aggregates. Moreover, simple hydrophobic effects cannot be invoked as the only determinants of the amyloidogenic potential of a certain sequence. Very fine tuned molecular recognition factors, mainly linked to aromatic–aromatic interactions, appear to determine the amyloid properties of aggregating peptides. Substitution of Phe to Ala experimentally was observed to still yield partially ordered fibrils, and the results of our simulations make us hypothesize a different mechanism based on the fact the Ala is a good β-sheet former and is not so sterically hindering as to prevent two chains to become close to establish productive hydrogen bonding interactions. However, two Ala substitutions in a peptide at least 8-residue long are needed to still obtain a stable β-sheet complex in MD simulations.

This specificity of the interactions that are required to obtain an ordered β-sheet complex that may lead to the growth of fibrils puts severe restraints on the aggregation tendency of natural polypeptides under physiological conditions. The cases that we have presented here are clear examples where a simple hydrophobic collapse cannot account for the formation of an ordered amyloid fibril. On the contrary, very specific intermolecular recognition is needed to determine the final ordered supramolecular structure. Our results actually suggest that the formation and stabilization of oligomers formed by small peptides is highly dependent on the establishment of a sufficient number of specific contacts among side-chains at specific sequence positions.

From a practical point of view, our study suggests that MD simulation of minimal model peptides can be a very promising approach to complement experiments in order to solve the problem of rational control over the design of macromolecular architectures. Analyzing the fine chemical details underlying the molecular recognition process could be helpful in designing new capping peptides able to bind to target sequences. Theoretical studies like the ones presented here can pinpoint and allow control on a wide set of variables, such as sequence, stereochemistry, solvent conditions, with the final goal of rationally designing and optimizing new peptides for amyloid-like polymerization [10], leads for amyloid breaking [42,43] and peptide-based molecules for material science and nanotechnology [44].

References

[1] J.C. Rochet, P.T. Landsbury Jr., Amyloid fibrillogenesis: themes and variations, Curr. Opin. Struct. Biol. 10 (2000) 60–68.
[2] C.M. Dobson, Protein misfolding, evolution and disease, Trends Biochem. Sci. 4 (1999) 989–998.
[3] P.T. Jarrett, P.T. Lansbury Jr., Amyloid fibril formation requires a chemically discriminating nucleation event: studies of an amyloidogenic sequence from the bacterial protein OsmB, Biochemistry 31 (1992) 12345–12352.
[4] J.I. Guijarro, M. Sunde, J.A. Jones, I.D. Campbell, C.M. Dobson, Amyloid fibril formation by an SH3 domain, Proc. Natl. Acad. Sci. U.S.A. 95 (1998) 4224–4228.
[5] M. Fandrich, M.A. Fletcher, C.M. Dobson, Amyloid fibrils from muscle myoglobin, Nature 410 (2001) 165–166.
[6] M.R. Chapman, L.S. Robinson, J.S. Pinkner, R. Roth, J. Heuser, M. Hammar, S. Normark, S.J. Hultgren, Role of *Escherichia coli* curli operons in directing amyloid fiber formation, Science 295 (2002) 851–855.
[7] D. Claessen, R. Rink, W.D. Jong, J. Siebring, P. de Vreugd, F.G.H. Boersma, L. Dijkhuizen, H.A.B. Wosten, A novel class of secreted hydrophobic proteins is involved in aerial hyphae formation in *Streptomyces coelicolor* by forming amyloid-like fibrils, Genes Dev. 17 (2003) 1714–1726.
[8] E. Gazit, The "Correctly Folded" state of proteins: is it a metastable state? Angew. Chem. Int. Ed. Engl. 41 (2002) 257–259.
[9] M. Lopez de la Paz, L. Serrano, Sequence determinants of amyloid fibril formation, Proc. Natl. Acad. Sci. U.S.A. 101 (2004) 87–92.

[10] M. Lopez de la Paz, K. Goldie, J. Zurdo, E. Lacroix, C.M. Dobson, A. Hoenger, L. Serrano, De novo designed peptide-based amyloid fibrils, Proc. Natl. Acad. Sci. U.S.A. 99 (2002) 16052–16057.
[11] P. Hammarstrom, X. Jiang, A.R. Hurshman, E.T. Powers, J.W. Kelly, Sequence-dependent denaturation energetics: a major determinant in amyloid disease diversity, Proc. Natl. Acad. Sci. U.S.A. 99 (2002) 16427–16432.
[12] B. Ciani, E.G. Hutchinson, R.B. Sessions, D.N. Woolfson, A designed system for assessing how sequence affects alpha to beta conformational transitions in proteins, J. Biol. Chem. 277 (2002) 10150–10155.
[13] B.Y. Ma, R. Nussinov, Stabilities and conformations of Alzheimer's beta-amyloid peptide oligomers (Aβ(16–22) Aβ(16–35) and Aβ(10–35)): sequence effects, Proc. Natl. Acad. Sci. U.S.A. 99 (2002) 14126–14131.
[14] I. Daidone, F. Simona, D. Roccatano, R.A. Broglia, G. Tiana, G. Colombo, A.D. Nola, Beta-hairpin conformation of fibrillogenic peptides: structure and alpha–beta transition mechanism revealed by molecular dynamics simulations, Proteins: Struct. Funct. Bioinform. 57 (2004) 198–204.
[15] N. Mousseau, P. Derreumaux, Exploring the early steps of amyloid peptide aggregation by computers, Acc. Chem. Res. 38 (2005) 885–891.
[16] J. Gsponer, U. Haberthur, A. Caflisch, The role of side-chain interactions in the early steps of aggregation: molecular dynamics simulations of an amyloid-forming peptide from the yeast prion Sup35, Proc. Natl. Acad. Sci. U.S.A. 100 (2003) 5149–5154.
[17] S. Gnanakaran, R. Nussinov, A.E. Garcia, Atomic level description of amyloid beta-dimer formation, J. Am. Chem. Soc. 128 (2006) 2158–2159.
[18] G. Colombo, I. Daidone, E. Gazit, A. Amadei, A. Di Nola, Molecular dynamics simulation of the aggregation of the core-recognition motif of the islet amylolid polypeptide in explicit water, Proteins: Struct. Funct. Bioinform. 59 (2005) 519–527.
[19] H.D. Nguyen, C.K. Hall, Spontaneous fibril formation by polyalanines; discontinuous molecular dynamics simulations, J. Am. Chem. Soc. 128 (2006) 1890–1901.
[20] A. Melquiond, G. Boucher, N. Mousseau, P. Derreumaux, Following the aggregation of amyloid-forming peptides by computer simulations, J. Chem. Phys. 122 (2005) 174904.
[21] G.G. Tartaglia, A. Cavalli, R. Pellarin, A. Caflisch, Prediction of aggregation-prone segments in polypeptide sequences, Protein Sci. 14 (2005) 2723–2734.
[22] D.V. Klimov, J.E. Straub, D. Thirumalai, Aqueous urea destabilizes Aβ(16–22) oligomers, Proc. Natl. Acad. Sci. U.S.A. 101 (2004) 14760–14765.
[23] D. Zanuy, R. Nussinov, The sequence dependence of fiber organization. A comparative molecular dynamics study of the Islet Amyloid Polypeptide Segments 22–27 and 22–29, J. Mol. Biol. 329 (2003) 565–584.
[24] D. Zanuy, Y. Porat, E. Gazit, R. Nussinov, Peptide sequence and amyloid formation; molecular simulations and experimental study of a human islet amyloid polypeptide fragment and its analogs, Structure 12 (2004) 439–455.
[25] D. Zanuy, N. Haspel, H.H. Tsai, B.Y. Ma, K. Gunasekaran, H.J. Wolfson, R. Nussinov, Side chain interactions determine the amyloid organization: a single layer beta-sheet molecular structure of the calcitonin peptide segment 15–19, Phys. Biol. 1 (2004) 89–99.
[26] M. Lopez de la Paz, G.M.S. De Mori, L. Serrano, G. Colombo, Sequence dependence of amyloid fibril formation: insights from molecular dynamics simulations, J. Mol. Biol. 349 (2005) 583–596.
[27] M. Reches, E. Gazit, Amyloidogenic hexapeptide fragment of medin: homology to functional islet amyloid polypeptide fragments, Amyloid: J. Protein Fold. Disord. 11 (2004) 81–89.
[28] A. Naito, M. Kamihira, R. Inoue, H. Saito, Structural diversity of amyloid fibril formed in human calcitonin as revealed by site-directed 13C solid-state NMR spectroscopy, Magn. Reson. Chem. 42 (2004) 247–256.
[29] O.S. Makin, E. Atkins, P. Sikorski, J. Johansson, L.C. Serpell, Molecular basis for amyloid fibril formation and stability, Proc. Natl. Acad. Sci. U.S.A. 102 (2005) 315–320.
[30] H. Inouye, D. Sharma, W.J. Goux, D.A. Kirschner, Structure of core domain of fibril-forming PHF/Tau fragments, Biophys. J. 90 (2006) 1774–1789.
[31] G. Mucchiano, G.G. Cornwell III, P. Westermark, Senile aortic amyloid. Evidence for two distinct forms of localized deposits, Am. J. Pathol. 140 (1992) 811–877.
[32] R. Nelson, M.R. Sawaya, M. Balbirnie, A.O. Madsen, C. Riekel, R. Grothe, D. Eisenberg, Structure of the cross-beta spine of amyloid-like fibrils, Nature 435 (2005) 773–778.
[33] H.J.C. Berendsen, J.R. Grigera, T.P. Straatsma, The missing term in effective pair potentials, J. Phys. Chem. 91 (1987) 6269–6271.
[34] B. Hess, H. Bekker, J.G.E.M. Fraaije, H.J.C. Berendsen, A linear constraint solver for molecular simulations, J. Comp. Chem. 18 (1997) 1463–1472.
[35] S. Miyamoto, P.A. Kollman, SETTLE: an analytical version of the SHAKE and RATTLE algorithms for rigid water models, J. Comp. Chem. 13 (1992) 952–962.
[36] H.J.C. Berendsen, J.P.M. Postma, W.F. van Gunsteren, A.D. Nola, J.R. Haak, Molecular dynamics with coupling to an external bath, J. Chem. Phys. 81 (1984) 3684.
[37] H.J.C. Berendsen, D. van der Spoel, R. van Drunen, GROMACS: a message passing parallel molecular dynamics implementation, Comput. Phys. Commun. 91 (1995) 43–56.
[38] E. Lindahl, B. Hess, D. van der Spoel, Gromacs 3.0: a package for molecular simulation and trajectory analysis, J. Mol. Model. 7 (2001) 306–317.
[39] W.F. van Gunsteren, X. Daura, A.E. Mark, GROMOS force field, Encyclopedia Comp. Chem. 2 (1998) 1211–1216.
[40] X. Daura, B. Jaun, D. Seebach, W.F. van Gunsteren, A.E. Mark, Reversible peptide folding in solution by molecular dynamics simulation, J. Mol. Biol. 280 (1998) 925–932.
[41] D.J. Gordon, J.J. Balbach, R. Tycko, S.C. Meredith, Increasing the amphiphilicity of an amyloidogenic peptide changes the beta-sheet structure in the fibrils from antiparallel to parallel, Biophys. J. 86 (2004) 428–434.
[42] M. Pickhardt, Z. Gazova, M.V. Bergen, I. Khlistunova, Y.P. Wang, A. Hascher, E.M. Mandelkow, J. Biernat, E. Mandelkow, Anthraquinones inhibit tau aggregation and dissolve Alzheimer's paired helical filaments *in vitro* and in cells, J. Biol. Chem. 280 (2005) 3628–3635.
[43] S. Taniguchi, N. Suzuki, H. Masuda, S. Hisanaga, T. Iwatsubo, M. Goedert, M. Hasegawa, Inhibition of heparin-induced tau filament formation by phenothiazines, polyphenols and porphyrins, J. Biol. Chem. 280 (2005) 7614–7623.
[44] M. Reches, E. Gazit, Casting metal nanowires within discrete self-assembled peptide nanotubes, Science 300 (2003) 625–627.